

# Voltage imbalance compensation using synchronous compensator with multivariable filter in microgrids

Alireza Mohammadi Amidi<sup>1,5,\*</sup> , Pooya Parvizi<sup>2</sup> , Milad Jalilian<sup>3,5</sup> ,  
Hana Parvizi<sup>4</sup> 

<sup>1</sup>Department of Electrical Engineering, Razi University, Kermanshah, Iran.

<sup>2</sup>Department of Mechanical Engineering, University of Birmingham, Edgbaston, Birmingham, UK.

<sup>3</sup>Department of Physics, Faculty of Science, Lorestan University, Khorramabad, Iran.

<sup>4</sup>Department of Science, University of British Columbia, Vancouver, Canada.

<sup>5</sup>Pooya Power Knowledge Enterprise, Tehran, Iran.

\*Corresponding author: [alireza.moamidi@gmail.com](mailto:alireza.moamidi@gmail.com)

## Original Research

## Abstract:

Received:  
22 August 2024  
Revised:  
20 October 2024  
Accepted:  
3 November 2024  
Published online:  
15 December 2024

© The Author(s) 2024

Unbalanced voltage is a prevalent issue in power networks that can have significant adverse effects. Voltage unbalance arises when the three-phase voltages in the power system differ in magnitude or phase angle, leading to waveform distortion. This imbalance can increase energy losses, thereby elevating costs for energy consumers. Additionally, it can negatively impact the power factor, which measures the efficiency of power usage in the system. To improve power quality and mitigate the detrimental effects, this paper proposes an innovative control strategy using a Static Synchronous Compensator (STATCOM) based on the multivariable filter (MVF) method within a utility-connected microgrid. The MVF configuration effectively separates the positive and negative components, which are then utilized in control loops. First, the voltage control loop builds the references for current control loop. Then, the current control unit sends the appropriate commands to the STATCOM in order to compensate the voltage amplitude. The primary advantage of the proposed strategy is its precision in reference tracking and ease of implementation. The MVF-based STATCOM can compensate for voltage imbalances by injecting reactive power and regulating the DC-link voltage. The results demonstrate that the proposed control structure effectively eliminates negative components and enhances the voltage profile of the studied microgrid.

**Keywords:** Unbalanced voltage compensation; Multivariable filter; Static synchronous compensator; Microgrids

## 1. Introduction

Power grids face numerous problems such as the reduction of fossil resources, low energy efficiency, and environmental pollution all over the world. These vexingly complicated issues have increased the tendency to generate power at the distribution voltage level. The resources used in distributed generation include natural gas, biogas, wind energy, photovoltaic cells, fuel cells, cogeneration of heat and power (CHP), micro-turbines, Stirling engines, and a combination of mentioned resources. This type of power generation at the level of distribution networks is called distributed generation (DG) and the distributed generation resources

are well-known as DERs. The reason for this naming is to differentiate between these resources and conventional large power plants. With the integration of DG sources, traditional distribution networks become active networks [1, 2].

Distributed generation in the general sense refers to any type of production at the place of consumption. Different countries and institutions have provided various definitions for distributed generation. In other words, the power delivery area of DG units is a source of energy generation directly linked to the distribution network [3]. Microgrids are small-scale networks at low voltage levels that feed thermal and

electrical loads in small regions such as houses, schools, universities, and commercial and economic areas with the help of cutting-edge technologies. Since the microgrids are composed of DG sources and different types of loads at the level of distribution voltage, they are included in the active distribution networks [4, 5]. Flexibility in microgrids makes it possible to act as an independent controlled unit and to have the ability to connect to the main grid to meet the reliability and power quality requirements of the covered areas as well as the main grid [6].

The extensive use of non-linear and single-phase loads as well as power electronic devices in electrical systems has resulted in voltage imbalance, voltage harmonics, and distortion of the main voltage components, which are the common issues in the power quality subject. These challenges can increase system losses and also bring adverse effects such as malfunctioning of variable speed drives and protective relays, overheating of motors and transformers, and power factor correction capacitor errors. The importance of the power quality problem becomes more prominent when there may be sensitive loads in a power grid that require high power quality, and as a result, the maximum amount of disturbance allowed for them is low [7, 8].

Many studies have been conducted on unbalanced voltage compensation in microgrids in recent decades. Controllers based on smart algorithms [9, 10], adaptive methods [11, 12], droop controllers [13, 14], and ESS-based approaches are some of the strategies discussed voltage imbalance compensation in the literature.

One of the most effective tools in combating the unbalanced voltage conditions in microgrids is Flexible Alternative Current Transmission Systems (FACTS) devices. These units can significantly improve power quality and eliminate voltage imbalance when they are equipped with powerful control systems [15]. Key FACTS devices include Static Var Compensators (SVC) and Static Synchronous Compensators (STATCOM) for fast reactive power compensation and voltage support [16]. Thyristor-Controlled Series Capacitors (TCSC) and Static Synchronous Series Compensators (SSSC) modulate reactance to control power flow and improve stability [17]. Unified Power Flow Controllers (UPFC) and Interline Power Flow Controllers (IPFC) manage real and reactive power flows in transmission lines [18]. Dynamic Voltage Restorers (DVR) protect sensitive loads from voltage disturbances, while Phase-Shifting Transformers (PST) and Thyristor-Controlled Phase Shifting Transformers (TCPST) adjust phase angles for power flow control [19]. Advanced Series Compensation (ASC) combines series capacitors and power electronics to dynamically enhance power flow and stability. These devices collectively improve voltage profiles, reduce transmission losses, and support the integration of renewable energy sources [20]. STATCOM, is a parallel FACTS device generating a balanced set of three-phase sinusoidal voltages at base frequency, and capable of expeditious control mechanism on amplitude and phase angle [21, 22]. This tool is able to provide unbalanced voltage compensation. To adjust the point of common coupling (PCC) voltage, STATCOM tries to manage reactive power. In other words, when the required

voltage level is higher than the grid voltage, the STATCOM produces reactive power to elevate the voltage level precisely. Furthermore, when the required voltage level is lower than the grid voltage, this compensation device consumes the precise amount of reactive power to decrease the voltage and reach the desired level [23]. On the other hand, the presence of power electronic converters (PECs) in the configuration of STATCOM enables the potential of delivering active/reactive power and deal with voltage balancing issues [24, 25].

Employing STATCOM under balanced conditions has been investigated by many researchers. In [26], the voltage regulation objective with STATCOM based on genetic algorithm (GA) optimization was explored under different operating conditions. It was shown that dampening fluctuations, and increasing the microgrid's overall stability could be achieved using optimally controlled STATCOM equipment. Compensating the lack of reactive power in a microgrid by means of an optimized STATCOM has been presented in [27]. The results indicated that by tuning the STATCOM device parameters with meta-heuristic algorithms such as particle swarm optimization (PSO), the required amount of reactive power to create balance in a microgrid is feasible. Another study [28] investigates the voltage control in an isolated hybrid power system. In this study, the focus of implementing STATCOM was on delivering the exact amount of reactive power needed for meeting the power system demands and enhancing voltage stability. Also, the mine blast optimization has been applied to the proposed STATCOM to obtain more precise results. In [29], a STATCOM was combined with a fuzzy logic controller (FLC) to achieve more stability, improved voltage profile, less power loss, and power flow regulation. It was witnessed that the integration of STATCOM with fuzzy control systems led to higher distribution line capacity, loss reduction, and better voltage profile simultaneously. Furthermore, mitigating voltage fluctuation and correcting the power factor have been experimented with by exploiting STATCOM configuration in a microgrid. The objectives of this paper were to keep the oscillations in the allowed range and reach a standard level of voltage regulation. The results confirmed the suggested STATCOM was able to cooperate in the process of creating balance and stabilization of the island microgrid [30].

On the other hand, recently, a great number of strategies have been presented with the aim of unbalanced voltage compensation via STATCOMs, mostly concentrated on positive and negative component separation. In [31], a novel control system has been considered for cascade STATCOMs under unbalanced conditions. The STATCOMs were star-connected to the power supply to generate positive/negative components. Using the proposed control approach, DC-link stability and reference current tracking could be highly attainable. But, the debatable challenge of this method is that it has a complex structure. Also, in [32, 33], dynamic phasor (DP) modeling has been exploited in unbalanced microgrids integrated with STATCOMs using the ABC reference frame.

From the perspective of double reference frames, double synchronous reference frames (DSRF), and decoupled dou-

ble synchronous reference frames (DDSRF) have been explored in STATCOM-related studies. DSRF is a method, which can separate the positive and negative components using a stationary  $d - q$  frame. Through this approach, oscillations with a frequency twice the fundamental frequency are extracted and can be eliminated via a suitable control system. Reference [34] proposed an effective control scheme for both PCC voltage fluctuation dampening and improving the system reliability using DSRF-based STATCOM in the  $d - q$  frame. The main goal of the paper was to separately control positive, negative and zero components under the unbalanced circumstances. The simulation results verified the proper performance of the suggested control system in both normal and abnormal condition. It was also demonstrated that the proposed structure could enhance the power quality and attenuate overcurrent associated with the STATCOM. A notable issue of the DSRF separation technique is that when using this method, the coupling effects between sequence components will not be completely eliminated and thus the output signals are not purely DC, containing oscillations [35]. Hence, the DDSRF approach has gained more attention within the sequence separation studies. In [36], unbalanced voltage sag mitigation through reactive power injection by means of Lab-scaled STATCOM has been investigated in a weak grid. The control system was equipped with a DDSRF approach to segregate the positive and negative components caused by unbalanced conditions. The results guaranteed the performance of the 2 kVA, 220 V DDSRF-based STATCOM in the terms of attenuation of voltage fluctuations and increasing the overall system stability. Another important study [37], has inquired into implementing a STATCOM combined with a DDSRF technique besides a fast-acting DC-link control system in a microgrid. The suggested control strategy enabled the capability of positive/negative independent control loops. In addition to unbalanced PCC voltage compensation, the DC-link control scheme was also presented in this paper. The unbalanced condition was simulated via MATLAB software and the simulation outcomes validated the voltage imbalance compensation and appropriate functionality of the DC-link control system in the microgrid. Also, a fast recovery of voltage amplitude can be achievable within the proposed configuration. Comprehensive research has been conducted in [38], investigating various sequence separation methods implemented on STATCOM with single delta bridge cell-modular multilevel converters structure under grid oscillations. It was proved that DDSRF technique is more precise than the other strategies in purifying DC output signals and suppressing the fluctuations. On the other hand, the DDSRF method is complicated and implies too much computational burden to the system. Considering this limitation, there is an urgent need for a less complex technique with the equal precision of the DDSRF approach. Hence, a multivariable filter (MVF) is utilized in this paper. MVF simply positive/negative components would be simply separated with low oscillations. This way, the STATCOM control system linked with the separation technique will be easier to implement and faceless complexity. Another advantage of MVF is that the fundamental basis of this filter

relies on extracting the essential components exactly  $\alpha\beta$  within the frame.

The main contribution of the paper can be listed as follows:

- \* The proposed STATCOM combined with MVF approach is consistently powerful in performance and holds less complexity compared to previous techniques.
- \* Voltage imbalance at PCC is compensated while maintaining effective DC-link control, even under unbalanced conditions.
- \* Reactive power is injected to regulate AC voltage through a multivariable filter, which is integrated with both voltage and current control loops.

The rest of the paper is organized as follows. Section 2 presents the system under study. The proposed control structure is given in section 3. Section 4 discusses the results and finally, section 5 give the conclusion.

## 2. System under study

A microgrid operating in grid-connected mode is considered in this study. The schematic of the microgrid alongside the general components, and the STATCOM is presented in Fig. 1. As can be observed from the figure, an unbalanced load is connected to the STATCOM-based microgrid. The MVF is utilized for separating the positive and negative sequence components. The positive and negative components are received by the voltage control loop used for compensation purposes, which generates control signals for the reference current. The current control loop configuration is employed to manage the current of the VSC. The detailed model of the proposed system, including LC filter, MVF, Inverter STATCOM, line parameters and control system gains, is shown in Fig. 2. The parameters and specifications are given in Table 1.

## 3. Proposed control technique

### 3.1 MVF

In an unbalanced STATCOM, the voltage and current waveforms of the different phases may not be identical, which can cause problems such as power quality issues, unbalanced power flows, and potential equipment damage. In other words, imbalance, as one of the inevitable problems of STATCOM, should be compensated. The first step in the compensation process is to separate positive and negative sequence components. In unbalanced conditions, assume that the three-phase unbalanced current is as follows:

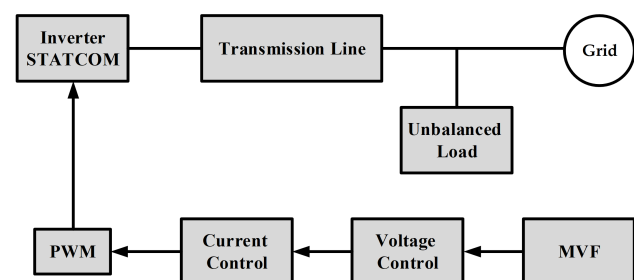
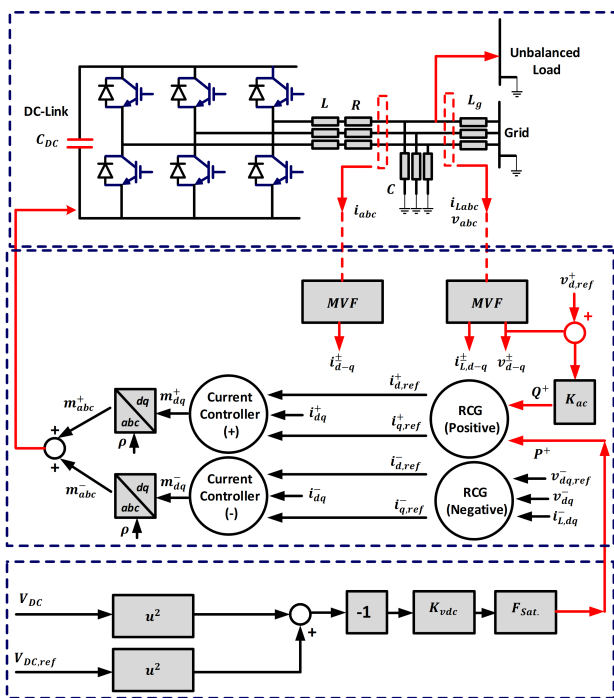


Figure 1. A general schematic of utility-connected microgrid including DDSTF-based STATCOM.

**Table 1.** Parameters and specifications [39].

Parameters	Symbol	Value
Voltage	$V$	391 [V]
Power (Inverter)	$P$	2000 [kW]
Capacitance (DC Link)	$C_{DC}$	9812 [ $\mu$ F]
Initial DC Link Voltage	$V_{DC,int}$	1500 [V]
Capacitance (Inverter Filter)	$C$	2500 [ $\mu$ F]
Rated Angular Frequency	$\omega_0$	377 [rad/s]
Inductance (Inverter Filter)	$L$	100 [ $\mu$ H]
Resistance (Inverter Filter)	$R$	1.19 [m $\Omega$ ]
Grid Inductance	$L_g$	50 [ $\mu$ H]
Line Impedance	$Z$	0.01+3.7j
Notch Filter Frequency	$f_n$	120 [Hz]
Switching Frequency	$f_s$	3 [kHz]
Negative Voltage controller	$K_{d,q-v}^-$	1.6
Current controller coefficients	$K_{d,q-i}^\pm$	Proportional: 0.2 Integral: 4.14
DC-link controller coefficients	$K_{vdc}$	$1868 * \frac{s+19}{s(s++2077)}$
Positive Voltage controller	$K_{ac}$	2/s



**Figure 2.** The proposed STATCOM integrated with a grid-connected MG.

$$i_{abc} = i_{abc}^+ + i_{abc}^- \tag{1}$$

According to the clockwise and counter-clockwise rotation, the positive and negative components of the current in the  $d-q$  frame are as follows:

$$i_{dq}^+ = i_{dq}^+ \text{ DC term} + e^{-j(\theta^+ - \theta^-)} i_{dq}^- \text{ Oscillatory term} \tag{2}$$

$$i_{dq}^- = i_{dq}^- \text{ DC term} + e^{-j(\theta^- - \theta^+)} i_{dq}^+ \text{ Oscillatory term} \tag{3}$$

$$\theta^+ = \omega t + \varphi^+ \quad \theta^- = -\omega t + \varphi^- \tag{4}$$

In the above equation,  $\varphi^+$  and  $\varphi^-$  are initial phases of positive and negative sequence of current, respectively. According to the above equations in the  $d-q$  axis, oscillatory and dc components are created, and the frequency of the oscillatory components will be twice the network frequency. In the DSRF method, a low pass filter is used to remove fluctuations. However, this method cannot remove unbalanced fluctuations perfectly and causes errors in the controller performance.

Here, multivariate filter (MVF) is used to solve the aforementioned problem as well as to fix the defects and reduce the complexity of the previous works. A multivariable filter is a control system that can manipulate multiple variables simultaneously to achieve a desired outcome. In the context of unbalanced microgrids, a multivariable filter can be designed to regulate the voltage and current waveforms of all three phases of the grid simultaneously, taking into account the interdependence between them. This component-separating filter combined with STATCOM can compensate for the voltage imbalance, and attenuate the undesired fluctuations. The block diagram of the multivariate filter is shown in Fig. 3.

One of the most important advantages of the multivariate filter is its simple implementation. Multivariate filter relationships are as follows:

$$\hat{x}_\alpha = \frac{k}{s} [x_\alpha(s) - \hat{x}_\alpha(s)] - \frac{\omega}{s} x_\beta(s)$$

$$\hat{x}_\beta = \frac{k}{s} [x_\beta(s) - \hat{x}_\beta(s)] - \frac{\omega}{s} x_\alpha(s)$$

In these relationships,  $x$  represents voltage or current, and  $\hat{x}$  represents the output of the multivariate filter. In the above relation, we define the constant  $K$  to find the cutoff frequency of the multivariate filter. A smaller value of  $K$  leads to increased filter selectivity. To gain a deeper understanding of the effectiveness of MVF technique, see Appendix A.

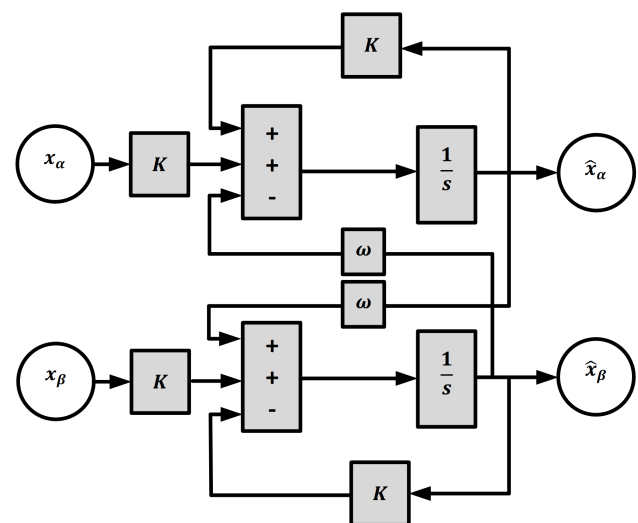


**Figure 3.** Schematic of Multivariable filter configuration.

### 3.2 Current controllers of positive and negative sequence components

In unbalanced STATCOM, the current controller is responsible for regulating the flow of current in the power converter that interfaces the STATCOM with the grid. The current controller is designed to ensure that the STATCOM injects the necessary reactive power to compensate for the unbalanced loads in the grid, and to maintain a stable voltage profile. The current controller in unbalanced STATCOM can be implemented using different control strategies, including PI control, sliding mode control, and model predictive control. The choice of control strategy depends on the specific requirements of the STATCOM and the performance objectives of the controller.

The mathematical relationships of the current controller in unbalanced STATCOM can be expressed using Kirchhoff's Voltage Law on the output inductance filter. Once these equations have been transformed into  $d - q$  frame:

$$L \frac{di_d^\pm(t)}{dt} + Ri_d^\pm(t) = v_{id}^\pm(t) - v_d^\pm(t) + L\omega_0 i_q^\pm(t) \quad (5)$$

$$L \frac{di_q^\pm(t)}{dt} + Ri_q^\pm(t) = v_{iq}^\pm(t) - v_q^\pm(t) - L\omega_0 i_d^\pm(t) \quad (6)$$

where,  $R$  and  $L$  are the output passive filter of STATCOM respectively.  $\omega_0$  is network frequency and  $v_t$  is terminal voltage of STATCOM and define as  $v_{idq}^\pm(t) = \frac{v_{DC}}{2} m_{dq}^\pm$ . The inclusion of term  $L\omega_0$  in Equations (5) and (6) creates a coupling between  $i_d$  and  $i_q$  in both the positive and negative sequence components. To decouple the dynamics, we use the relationship  $y_{d,q}(t) = v_{idq}(t) - v_{dq}(t) \pm L\omega_0 i_{dq}(t)$  in Equations (5) and (6). By transforming these equations into the Laplace domain, we obtain  $Li_{d,q}^\pm(s) = -Ri_{d,q}^\pm(s) + y_{d,q}^\pm$ . In general, the current controller of a STATCOM adjusts the output of the system to respond to current changes in each phase. This adjustment is typically done using a control algorithm such as PI (Proportional-Integral). Once the control scheme has been selected, the next step is to determine the controller parameters. For a PI controller, the two main parameters are the proportional gain ( $k_p$ ) and integral gain ( $k_i$ ).

The PI control design takes into account the closed-loop model of the positive and negative current components. As illustrated in the schematics shown in Fig. 4, we would have  $K_{d,q-i}^\pm = k_p + \frac{k_i}{s}$ .

The design of the PI control involves considering the functional schematics of the closed-loop model for the positive and negative current components. These schematics are shown in Fig. 4. According to this figure, the transfer func-

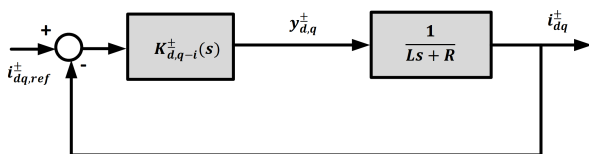


Figure 4. Schematic of current control loop.

tion of the open-loop system can be expressed as follows:

$$T_{ol}(s) = \left(\frac{k_p}{Ls}\right) \left(\frac{s + \frac{k_i}{k_p}}{s + \frac{R}{L}}\right) \quad (7)$$

Based on the aforementioned equation, the open-loop system's transfer function has a stable pole at point  $p = -\frac{R}{L}$ , which is somewhat close to the origin, resulting in a sluggish system response. To enhance the system's frequency response, the PI controller zero can nullify the pole. This allows for the closed-loop transfer function of the system to improve.

$$G_i(s) = \frac{i_{dq}^\pm(s)}{i_{dq,ref}^\pm(s)} = \frac{1}{\tau_i s + 1} \quad (8)$$

Equation (8) represents a transfer function of the first order. The time constant of the closed-loop control system, denoted by  $\tau_i$ , should be kept small to achieve a swift frequency response in the controller. Conversely, increasing  $\frac{1}{\tau_i}$  will significantly boost the closed-loop control system's bandwidth.

### 3.3 Voltage controller of positive and negative sequence components

The voltage controller in an unbalanced STATCOM is responsible for regulating the voltage of each phase of the system in order to balance the system and compensate for any voltage imbalances caused by unbalanced loads or other factors.

The voltage controller typically uses a PI (Proportional-Integral) control algorithm to adjust the output of the STATCOM in response to changes in the voltage of each phase. To design the voltage controller in the positive axis of the  $d - q$  frame, the momentary power theory should be used, and for the negative of the  $d - q$  frame, Kirchhoff's current law should be used.

Assuming the phase-locked loop (PLL) is in a stable condition, then. Consequently, active and reactive power in the  $d - q$  domain can be written.

$$P^+(t) = \frac{3}{2} [v_d^+(t) i_d^+(t)] \quad (9)$$

$$Q^+(t) = -\frac{3}{2} [v_d^+(t) i_q^+(t)] \quad (10)$$

$P^+$  and  $Q^+$  are controlled by  $i_d^+$  and  $i_q^+$  respectively, thus:

$$i_{dref}^+(t) = \frac{2}{3v_d^+} P^+(t) \quad (11)$$

$$i_{qref}^+(t) = \frac{-2}{3v_d^+} Q^+(t) \quad (12)$$

In Equation (11), the value of  $i_{dref}^+$  is obtained directly from the DC link controller (section 3-4). But in order to adjust the STATCOM output voltage, a voltage controller must be used in the positive axis. In Figure 2, the output voltage can be written as follows:

$$v_{abc}^+ = L_g \frac{di_{gabc}^+}{dt} + v_{gabc}^+ \quad (13)$$

In the above,  $v_{gabc}^+$  represents the three-phase grid voltage and  $i_{gabc}^+$  represents the grid current. Also  $L_g$  denote the grid inductance. According to the KCL law the grid current written as follow:

$$i_{gabc}^+ = i_{abc}^+ - i_{Labc}^+ \tag{14}$$

where  $i_{abc}^+$  is the output current of STATCOM and  $i_{Labc}^+$  is the load current. By transforming the above equation to the  $d-q$  frame:

$$v_d^+ = L_g \frac{di_{gd}^+}{dt} - L_g \omega_0 i_{gq}^+ + v_g^+ \tag{15}$$

$$v_q^+ = L_g \frac{di_{gq}^+}{dt} - L_g \omega_0 i_{gd}^+ + v_g^+ \tag{16}$$

In the positive axis, the value of  $v_q^+$  is zero, so its value can be ignored.

Figure 5 shows a control block diagram of the STATCOM voltage regulator and illustrates that a compensator  $K_{ac}$ , processes  $v_{d-ref}^+ - v_d^+$  and provides  $Q^+$ . Thus, an inspection of the control loop suggests that  $K_{ac}$  in its simplest form can be a proportional-integral (PI) compensator.

According to Figure 5, the plant transfer function is a simple gain, while  $K_{ac}$ , in its most basic form, acts as a PI compensator. Typically, the bandwidth of the closed-loop voltage control system is chosen to be significantly lower than that of the closed-loop current controllers, specifically,  $\frac{1}{\tau_i}$ .

On the other hand, as we said, to control the negative loop, we use Kirchoff's current law as follows:

$$C \frac{dv_d^-(t)}{dt} = i_d^-(t) - i_{Ld}^-(t) - C\omega(t)v_q^-(t) \tag{17}$$

$$C \frac{dv_q^-(t)}{dt} = i_q^-(t) - i_{Lq}^-(t) - C\omega(t)v_d^-(t) \tag{18}$$

where  $C$  is capacitance output filter of STATCOM. According to the above relations in the Laplace field, the PI controller should be used to make the voltage error zero in the steady state. For this purpose, the closed loop model of voltage control is presented in Fig. 6.

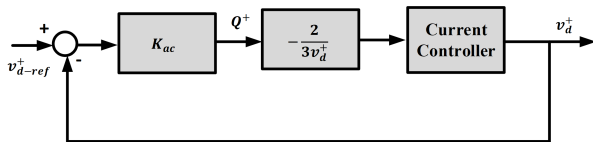


Figure 5. Control block diagram of the voltage regulator.

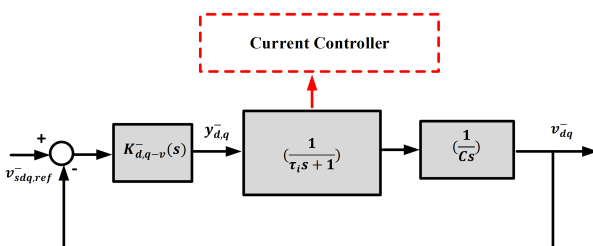


Figure 6. Closed loop model of voltage control system.

The open-loop voltage control system's transfer function has a coordinate-leading pole. Because of this, the closed-loop system has zero steady-state error, and as a result, the proportional-integral (PI) controller can be viewed as a proportional controller.

### 3.4 DC-link control

The DC link control in a STATCOM (Static Synchronous Compensator) is responsible for regulating the voltage and current in the DC link of the STATCOM. The DC link is the intermediate circuit that connects the AC side of the STATCOM to its DC side, and it is used to store and transfer energy between the two sides. The DC link control is crucial for the operation of the STATCOM, as it determines the amount of reactive power that the STATCOM can provide to the system. The DC link voltage must be maintained within a certain range in order to ensure that the STATCOM can operate properly and provide the required reactive power compensation.

The dynamic voltage of the DC link in a STATCOM is:

$$G_v(s) = \frac{v_{dc}^2}{P} = -\left(\frac{2}{C}\right) \frac{\tau s + 1}{s} \tag{19}$$

where,  $\tau$  is time constant and its relation is  $\tau = 2LP_{ext}/3v_{sd}^2$ . Fig. 7 depicts the block diagram of DC voltage regulations. The open-loop transfer function consists of three components: a compensator  $K_{vdc}(s)$ , a current controller  $G_i(s)$ , and a control plant  $G_v(s)$ :

$$l(s) = -K_{vdc}(s)G_i(s)G_v(s) \tag{20}$$

$l(s)$  denotes the open-loop transfer function. If we assume that  $K_{vdc}(s) = CH(s)/2s$  in Equation (20), then we get Equation (21) which states that

$$l(s) = G_i(s)H(s) \frac{\tau(s) + 1}{s^2} \tag{21}$$

In order to make sure that the phase delay caused by  $G_i$  is not significant, we set  $G_i$  equal to 1. If we define the frequency response, we can determine that the loop gain's magnitude becomes infinite as the control signal frequency increases. To implement a control strategy that has no steady-state errors, it is necessary to include the unstable poles of the Laplace transform in the compensator. Correspondingly:

$$H(s) = h \frac{s + \alpha}{s + \beta} \tag{22}$$

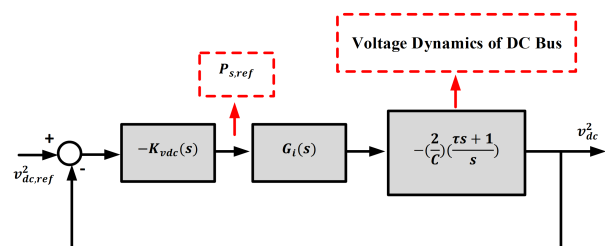


Figure 7. DC voltage compensation schematic.

Accordingly:

$$K_{vdc}(s) = h \frac{s + \alpha}{s(s + \beta)} \quad (23)$$

In above, the coefficients of the lead controller are represented by  $h$ ,  $\alpha$ , and  $\beta$ . To determine the controller coefficients based on the aforementioned equations,  $G_v(s)$  exhibits the largest phase lag when  $P_{ext}$  is at its maximum negative value. Ensuring an adequate phase margin at this operating point guarantees the closed-loop system's stability across other operating points. To design  $K_{vdc}(s)$ , the gain crossover frequency,  $\omega_c$ , is chosen to be sufficiently lower than the bandwidth of  $G_i(s)$ , allowing the assumption  $G_i(s) = 1 + j0$ . Subsequently,  $K_{vdc}(s)$  is designed to achieve a large phase margin under the worst-case operating condition. Notably,  $G_i(s)$ , as defined in Equation (20), is a first-order transfer function, making the root-locus design method a viable option. The root-locus method's advantage lies in its ability to directly relate performance indices, such as maximum overshoot and settling time, to the pole/zero loci, facilitating their consideration during the design process. For further information, refer to reference [39].

Finally, the detailed schematic of the proposed system can be seen in Fig. 2.

The DC-link control structure is responsible for stabilizing the DC-link voltage by adjusting the amount of power flowing between the microgrid and the utility grid. More importantly, the MVF-based STATCOM, which refers to a Static Synchronous Compensator (STATCOM) that uses a multivariable filter (MVF) method for voltage regulation and power factor correction in power systems, perfectly acts as a reactive power compensator combating voltage imbalance. It is to be noted that RCG stands for reference current generator and represents the saturation.

#### 4. Simulation and results

In this section, the system depicted in Fig. 2 is simulated using Simulink in MATLAB. Simulink provides an interactive graphical environment and a customizable set of block libraries that let you design, simulate, implement, and test a variety of time-varying systems, including communications, controls, signal processing, and more. Its tight integration with MATLAB makes it a powerful tool to model complex systems. Our Simulink model uses  $s$ -domain blocks for system definitions and Simulink solvers to simulate the  $t$ -domain responses.

The specifications of the system and the parameters of the control system are detailed in Table 1. This study explores two scenarios. The first scenario involves a comparative analysis where the conventional STATCOM control system is juxtaposed with the multivariate filter-based control system. This comparison aims to demonstrate the superior effectiveness of the multivariate filter over traditional methods, particularly in addressing imbalances. The second scenario examines the system's response to changes in reference values, showcasing the flexibility inherent in the proposed control approach.

rior effectiveness of the multivariate filter over traditional methods, particularly in addressing imbalances. The second scenario examines the system's response to changes in reference values, showcasing the flexibility inherent in the proposed control approach.

##### A) Scenario 1:

This scenario is designed to illustrate the effectiveness of the multivariate filter-based method (proposed method) in mitigating fluctuations and efficiently addressing voltage imbalances. The test system involves a STATCOM supplying a single-phase load connected to the grid, simulated using SimPowerSystems/Simulink. The primary goal is to showcase the efficacy of the proposed STATCOM (utilizing a multivariate filter) and validate its superiority in minimizing fluctuations and enhancing system stability compared to the conventional STATCOM.

At time  $t = 0.5$  s, a single-phase load with an impedance of  $0.01 + j7 \times 10^{-4}$  induces voltage imbalance in the test system. Fig. 8 depicts the waveform of the three-phase output voltage of the STATCOM under both the conventional control system and the proposed control scheme. Unbalanced voltage control loops are employed to address the

conventional STATCOM. At time  $t = 0.5$  s, a single-phase load with an impedance of  $0.01 + j7 \times 10^{-4}$  induces voltage imbalance in the test system. Fig. 8 depicts the waveform of the three-phase output voltage of the STATCOM under both the conventional control system and the proposed control scheme. Unbalanced voltage control loops are employed to address the

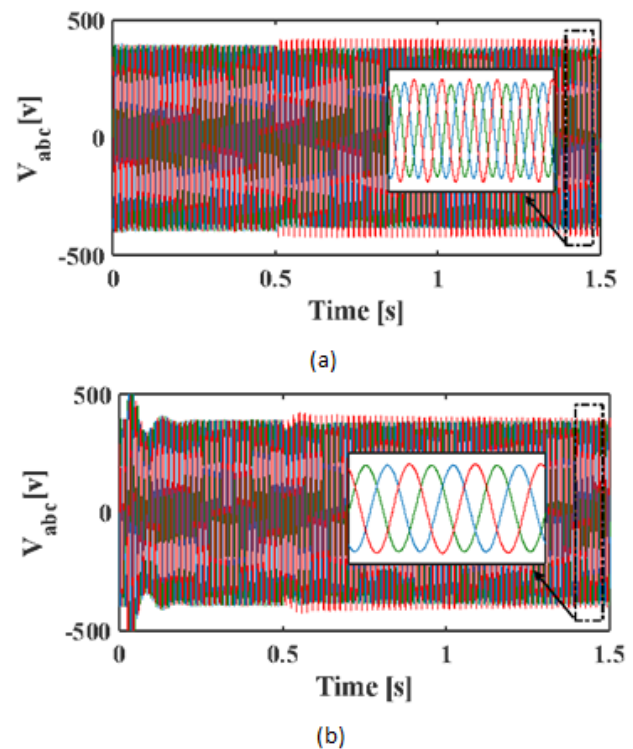


Figure 8. STATCOM output voltage (a) Conventional (b) Proposed.

Table 2. Simulation Scenarios.

DC link voltage reference is modified from 1500 V to 1700 V at $t = 0.5$ s
An unbalanced load is connected at $t = 0.8$ s
The three-phase voltage reference is altered from 391 V to 420 V at $t = 2.2$ s

imbalance. In the conventional control system, fluctuations hinder the compensation operation, leading to observable voltage imbalance. Conversely, the proposed control approach swiftly balances the voltage by applying accurate control commands to the inverter, ensuring stability in a short timeframe.

Figs. 9 and 10 depict the voltage of positive and negative components within the analyzed control systems. In situations of imbalance, the initial requirement is to segregate and regulate positive and negative components to rectify the imbalance. When unbalanced conditions occur and the transformation of three-phase voltage and current waves to the  $d-q$  frame is executed, mathematical relationships demonstrate the creation of oscillating components with a frequency of  $2\omega$  [35]. These disruptive fluctuations, generated during this transfer, adversely impact the control system's performance, leading to inadequate voltage compensation.

In the proposed strategy, a multivariate filter is employed to attenuate these fluctuations. Consequently, as illustrated in Figs. 9 and 10, the oscillations produced by the conventional method exhibit a frequency of  $2\omega$ , with a magnitude reaching 50 volts, causing disturbances in the system's behavior. Conversely, in the proposed method, not only has the separation of positive and negative components been effectively executed, but the  $2\omega$  fluctuations in this system have been significantly dampened. Within the proposed STATCOM structure, the magnitude of oscillations is restricted to less than 1 V, and there is notable precision in tracking the reference voltage.

Fig. 10 provides evidence that negative components on the

$dq$  axes in the conventional control system converge to 20 V and  $-15$  V, indicating minimal efforts to compensate for existing voltage imbalances in this control scheme. In contrast, it is observed that the use of the proposed control approach results in the negative values of the  $d-q$  axes reaching their reference (zero) over time.

#### B) Scenario 2:

The three-phase voltage diagram is illustrated in Fig. 11. In an ideal system, the voltage values in each phase should be equal, but in reality, they can vary due to various factors such as unbalanced loads and faulty equipment. At the beginning of the diagram there is no unbalanced load in the system but at  $t = 0.8$  s, when the unbalanced load is connected, it can be seen that there is a significant voltage imbalance between the three phases, with one phase having a much lower voltage than the other two. However, as time passes, the voltage in the low phase starts to increase, while the voltage in the other two phases decreases slightly. This indicates that the compensation process is working to balance the voltage across all three phases.

In a three-phase power system, the voltage can be analyzed in the  $d-q$  reference frame to separate the positive-sequence, and negative-sequence. The positive-sequence component represents the balanced three-phase voltage, while the negative-sequence component represents the unbalanced voltage. Fig. 12 and Fig. 13 clearly display the positive and negative voltage sequences in the  $d-q$  reference frame. The positive sequence voltage in the  $d$ -axis maintains a close alignment with its reference voltage range (391 – 420 V), while the positive component in the  $q$ -axis and the negative components in the  $d-q$  axis remain at

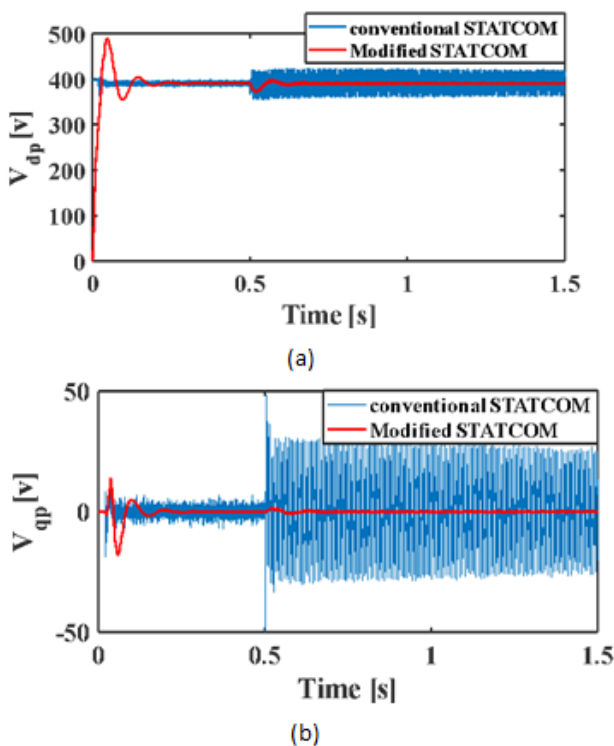


**Figure 9.** Output voltage positive component of STATCOM in  $d-q$  axis.

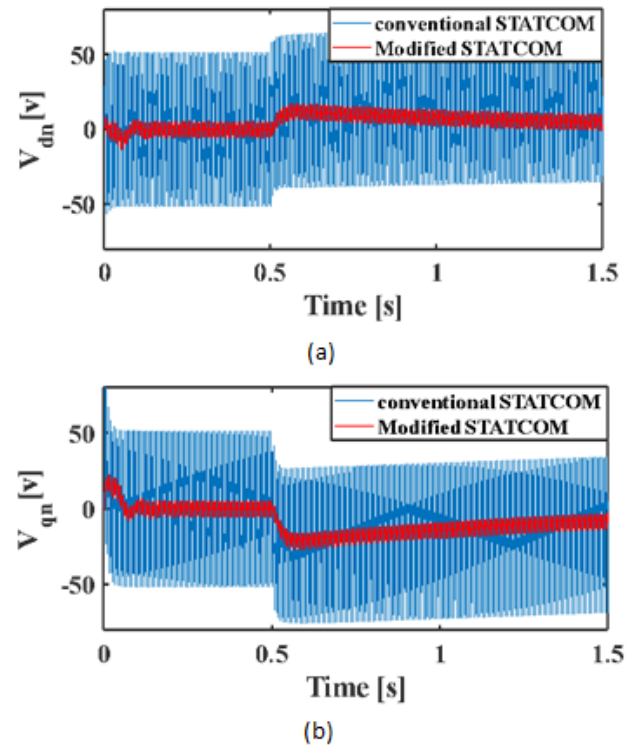
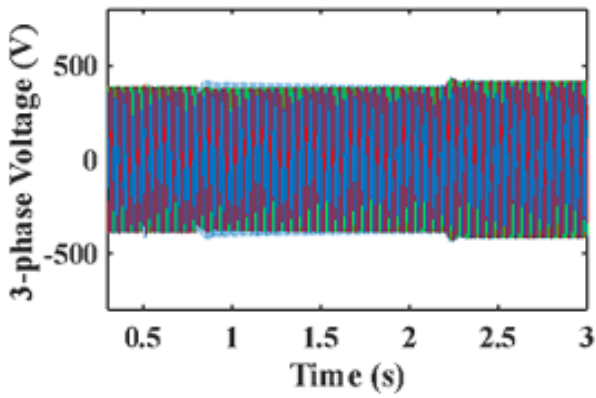
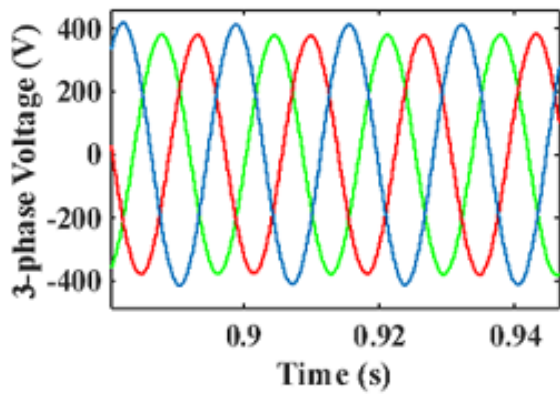


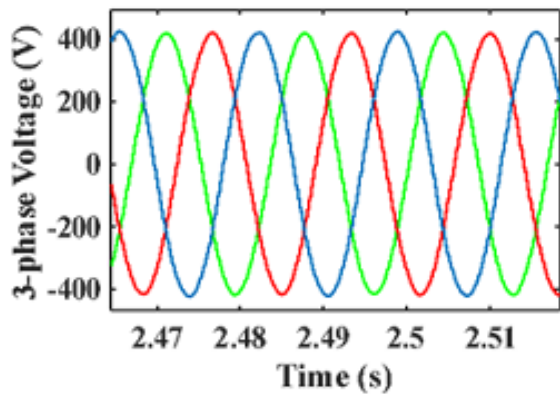
**Figure 10.** Output voltage negative component of STATCOM in  $d-q$  axis.



(a)



(b)



(c)

**Figure 11.** Voltage Compensation. (a) Three-phase voltage of STATCOM (b) Close look of unbalanced part (c) Close look of compensated part.

zero, indicating the accurate functioning of the inverter control system. Additionally, the amplitude of the negative sequence voltage in the  $d$  and  $q$  axes reduces effectively, which ensures that the VUF value remains within acceptable limits during steady-state operation.

The voltage unbalance factor (VUF) is an important parameter for assessing the quality of a three-phase power system. It represents the ratio of the negative-sequence voltage to the positive-sequence voltage and indicates the degree of voltage imbalance. Fig. 14 shows the VUF % for the PCC (Point of Common Coupling) voltage. As can be seen, at  $t = 0.8$ , the VUF value reaches around 7%, which

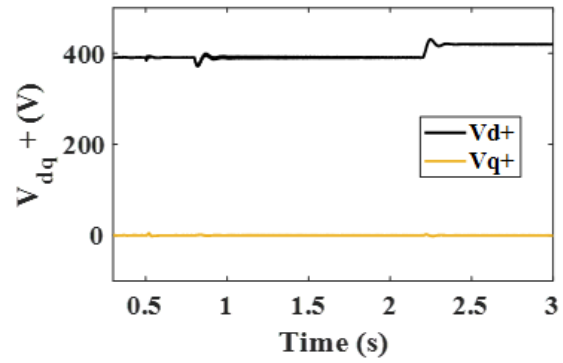


**Figure 12.** Voltage positive components for  $d - q$  frame.

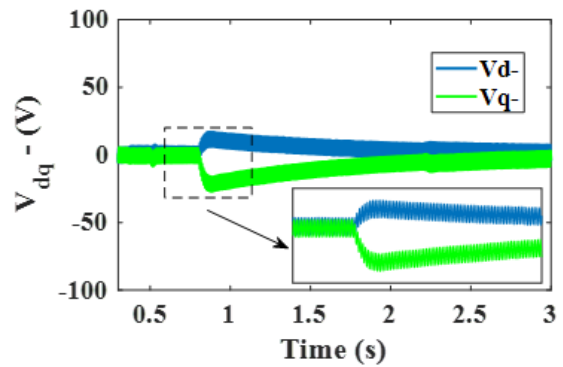


**Figure 13.** Voltage negative components for  $d - q$  frame.

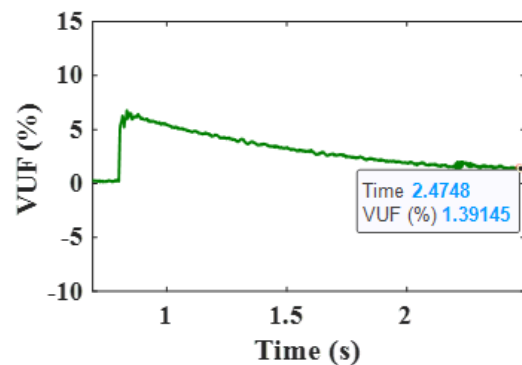


**Figure 14.** The percentage of voltage unbalance factor (VUF) within the simulation.

is significantly greater than the permitted value of 2%. This can lead to increased heating and reduced efficiency in the STATCOM, so it is important to monitor the VUF values and take corrective action if necessary to ensure the system operates safely and efficiently. As a result, the negative loop control system was employed to steadily decrease the VUF %, and at nearly  $t = 2.5$ , it entered the allowed range for the system, 1.39%. Overall, monitoring and controlling the VUF is critical for maintaining a healthy power system and preventing equipment damage.

On the other hand, the STATCOM DC link voltage diagram is given in Fig. 15. The DC capacitor and the control system that regulate the DC voltage. The DC capacitor stores the DC voltage that is converted from the AC input by the

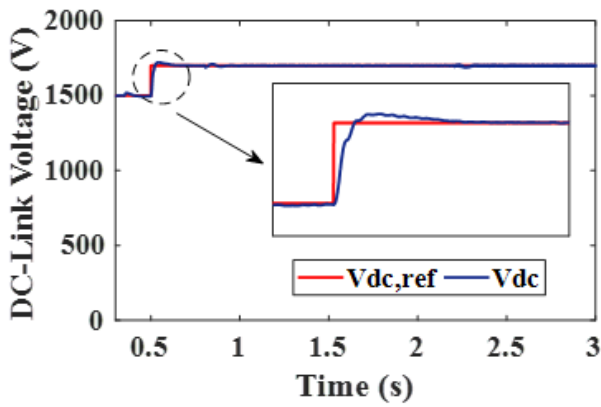


Figure 15. Schematic of DC-link voltage.

rectifier. The control system regulates the DC voltage to maintain it at a desired level, typically referred to as  $V_{dc,ref}$ . As shown in this figure, at  $t = 0.5$  seconds, the reference DC link voltage is increased stepwise from 1500 V to 1700 V. In response,  $K_{vdc}$  commands a positive  $P_{ref}^+$  to import real power from the AC system to the STATCOM DC side to increase  $V_{dc}$ . The figure demonstrates that  $V_{dc}$  is successfully regulated to  $V_{dc,ref}$ , with  $P_{ref}^+$  assuming small values that correspond to the STATCOM power loss.

Finally, the active and reactive power are taken into consideration. STATCOM is a device used for controlling reactive power and voltage in power systems. The STATCOM can inject or absorb reactive power into the system to regulate voltage levels, improve power factor, and stabilize the system. The active power, on the other hand, remains constant, as the device does not inject or absorb any active power. Fig. 16 depicts a line graph of the active and reactive power values for a STATCOM over a period of 3 seconds. The reactive power (green line) fluctuates over time, indicating that the STATCOM is continuously injecting or absorbing reactive power to regulate voltage levels in the system. The active power (blue line) remains constant at zero throughout the entire period, confirming that the device does not inject or absorb any active power. As shown in Fig. 16, the STATCOM can also provide reactive power to compensate for

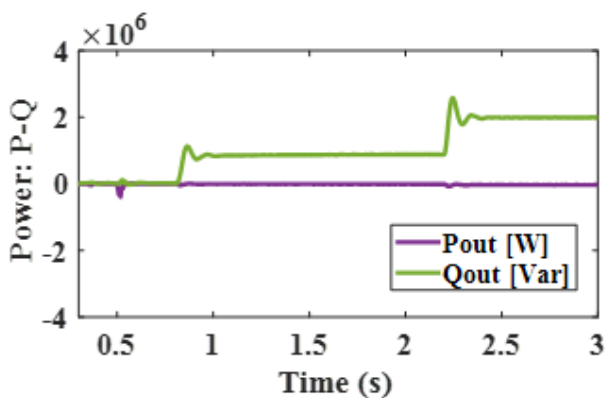


Figure 16. The amount of active-reactive power injecting via the STATCOM.

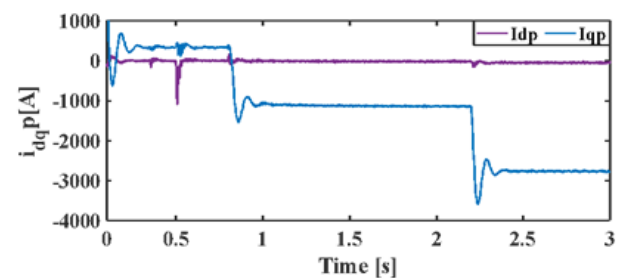
unbalanced loads and regulate PCC voltage. At  $t = 0.8$  seconds, an unbalanced load is added to the system, causing a voltage unbalance. The STATCOM control system responds by injecting approximately  $15 \times 10^5$  VAR of reactive power to compensate for the unbalanced voltage. At  $t = 2.2$  seconds, when the AC voltage reference changes from 391 V to 420 V, the STATCOM injects roughly  $20 \times 10^5$  VAR of reactive power to stabilize the PCC voltage.

In regard of current analysis, Fig. 17 (a) and 17 (b) illustrate the positive and negative components of the STATCOM output current along the  $d$  and  $q$  axes, respectively. These output waveforms are derived using the proposed method. As depicted in Fig. 17 (a), the positive  $d$ -axis current remains at zero across all scenarios, indicating that the STATCOM does not contribute to active power injection. Upon the appearance of an unbalanced load at the output of the STATCOM at  $t = 0.8$  s, the control system injects  $i_q^+$  to stabilize the voltage. This implies that reactive power is essential for maintaining voltage balance. Furthermore, at  $t = 2.2$  s in the second scenario, when the voltage reaches from 391 volts to 420 volts, the STATCOM control system enhances  $Q^+$  through the injection of  $i_q^+$ , thereby raising the output voltage.

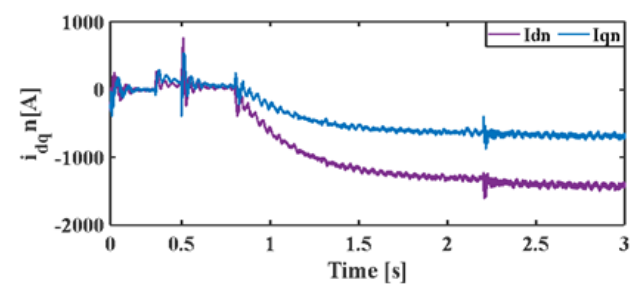
To address voltage imbalance, it is necessary to inject the negative component of the current into the network, as voltage balancing is achieved through this mechanism. Consequently, as shown in Fig. 17 (b), after addition of the unbalanced load, the current is introduced into the system through the negative  $d$  and  $q$  axes.

### 5. Comparison with previous methods

The performance and control strategies of STATCOM systems can vary significantly based on the methods employed. Conventional STATCOM systems typically rely on stan-



(a)



(b)

Figure 17. current positive and negative components for  $d - q$  frame.

standard control techniques, which often result in limited reliability and accuracy when dealing with voltage imbalances and reactive power compensation. In contrast, the DDSRF-based STATCOM (Double Decoupled Synchronous Reference Frame) and the MVF-based STATCOM (Multivariable Filter) offer enhanced reliability and accuracy. The DDSRF-based STATCOM employs a sophisticated approach that effectively decouples and manages the synchronous reference frames, allowing for precise control of reactive power and voltage stability. However, this increased complexity can make implementation and maintenance more challenging. On the other hand, the MVF-based STATCOM integrates a multivariable filter with voltage and current control loops, providing a simpler yet highly effective solution. The MVF-based system is less complicated than the DDSRF-based STATCOM while still offering superior control and performance compared to conventional systems. Additionally, both the DDSRF-based and MVF-based STATCOMs exhibit higher controllability than traditional STATCOM systems. This makes them more adept at maintaining system stability and efficiency under varying operating conditions. Table 3 presents a fair comparison between aforementioned techniques.

### 6. Possible future studies

Futuristic concepts could explore several advanced avenues. One potential area is the development of adaptive algorithms for multivariable filter tuning that respond to real-time changes in grid conditions, enhancing the STATCOM performance. Another research direction could involve integrating machine learning techniques to predict and mitigate voltage imbalances before they occur. Additionally, studies could focus on the scalability of such systems, examining how STATCOMs can be effectively implemented in larger or more complex microgrid configurations. The impact of renewable energy sources on voltage balance within the microgrid, and how STATCOMs can aid in maintaining stability despite the intermittent nature of these sources, is also a valuable field of study. Lastly, the economic and

environmental benefits of improved voltage balance, such as extended equipment life and reduced energy waste, could be quantified to justify investment in advanced STATCOM technologies.

### 7. Conclusion

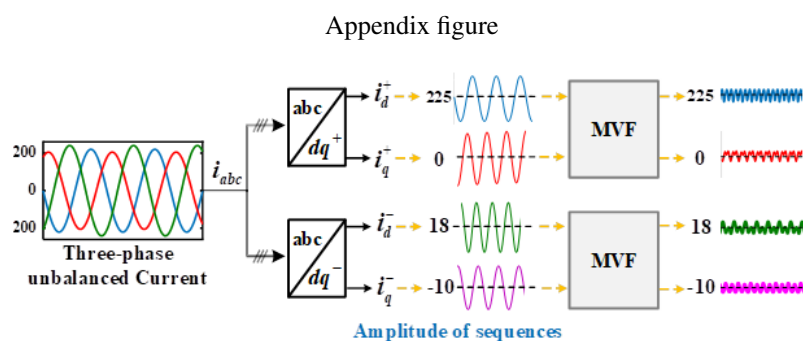
In this study, we presented a multivariable filter (MVF) integrated with STATCOM solution to mitigate unbalanced voltage conditions and improve power quality in a grid-connected microgrid. By separating the positive and negative voltage/current components using the MVF scheme, firstly, the voltage control loop plays its role to generate the current references. The generated signals are then used to create control commands for the STATCOM system within the current control loop. Then to show the resiliency of the suggested control system, a powerful control strategy for DC-link voltage was executed. Here, the conventional and proposed STATCOM configurations were compared to highlight the effectiveness of the multivariate filter-based method in mitigating fluctuations and efficiently addressing voltage imbalances. The results confirmed a significant reduction in the voltage unbalance factor (VUF) to its standard range, as well as effective control of active and reactive power. Specifically, by injecting reactive power, it was possible to compensate for the unbalanced voltage. This work demonstrates the high efficiency of the proposed approach for improving the performance and stability of grid-connected microgrids in the presence of voltage imbalance.

#### Appendix A:

Consider a scenario with an unbalanced three-phase current. In this case, the current amplitudes of the three phases are 200 A, 230 A, and 250 A, respectively. When this unbalanced current is transformed to the  $d - q$  axis, interesting patterns become evident, revealing both oscillatory and DC components. The exceptional effectiveness of the MVF approach is clearly demonstrated through its ability to mitigate these fluctuations, resulting in improved stability and control.

**Table 3.** A brief comparison between STATCOM voltage compensation strategies under unbalanced conditions.

Methods	Reliability	Controllability	Computational Burden
Conventional STATCOM	Low	Low	Low
DDSRF-based STATCOM	High	High	High
MVF-based STATCOM	High	High	Low



**Authors contributions**

All authors have contributed equally to prepare the paper.

**Availability of data and materials**

The data that support the findings of this study are available from the corresponding author upon reasonable request.

**Conflict of interests**

The authors declare that they have no known competing financial interests or personal relationships that could have appeared to influence the work reported in this paper.

**Open access**

This article is licensed under a Creative Commons Attribution 4.0 International License, which permits use, sharing, adaptation, distribution and reproduction in any medium or format, as long as you give appropriate credit to the original author(s) and the source, provide a link to the Creative Commons license, and indicate if changes were made. The images or other third party material in this article are included in the article's Creative Commons license, unless indicated otherwise in a credit line to the material. If material is not included in the article's Creative Commons license and your intended use is not permitted by statutory regulation or exceeds the permitted use, you will need to obtain permission directly from the OICC Press publisher. To view a copy of this license, visit <https://creativecommons.org/licenses/by/4.0>.

**References**

- [1] A. Muhtadi, D. Pandit, N. Nguyen, and J. Mitra. “**Distributed energy resources based microgrid: Review of architecture, control, and reliability**”. *IEEE Transactions on Industry Applications*, 57(3):2223–2223, 2021. DOI: <https://doi.org/10.1109/TIA.2021.306532>.
- [2] V. Nazari, M.H. Mousavi, and H. Moradi CheshmehBeigi. “**Reduction of Low Frequency Oscillations Using an Enhanced Power System Stabilizer via Linear Parameter Varying Approach**”. *Journal of Renewable Energy and Environment*, 9(2):59–74, 2022. DOI: <https://doi.org/10.30501/jree.2021.306909.1265>.
- [3] K. Prakash, A. Lallu, F.R. Slam, and K.A. Mammun. “**Review of power system distribution network architecture**”. In *2016 3rd Asia-Pacific World Congress on Computer Science and Engineering (APWC on CSE)*, pages 124–130, 2016. DOI: <https://doi.org/10.1109/APWC-on-CSE.2016.030>.
- [4] M. Ahmadi, M.H. Mousavi, and H. Moradi. “**Enhancing Resiliency in Standalone Microgrid Control System Using Consensus Algorithm Integrated with Multivariable Filter**”. In *2023 9th International Conference on Control, Instrumentation and Automation (ICCIA)*, pages 1–6, 2023. DOI: <https://doi.org/10.1109/ICCIA61416.2023.10506324>.
- [5] M.H. Mousavi and H. Moradi. “**Simultaneous compensation of distorted DC bus and AC side voltage using enhanced virtual synchronous generator in Islanded DC microgrid**”. *International Journal of Electronics*, pages 1–26, 2023. DOI: <https://doi.org/10.1080/00207217.2023.2278440>.
- [6] M. Soshinskaya, W.H. Crijns-Graus, J.M. Guerrero, and J.C. Vasquez. “**Microgrids: Experiences, barriers and success factors**”. *Renewable and sustainable energy reviews*, 40:659–672, 2014. DOI: <https://doi.org/10.1016/j.rser.2014.07.198>.
- [7] M.H. Mousavi, H.M. CheshmehBeigi, and M. Ahmadi. “**A DDSRF-based VSG control scheme in islanded microgrid under unbalanced load conditions**”. *Electrical Engineering*, 105(6):4321–4337, 2023. DOI: <https://doi.org/10.1007/s00202-023-01941-0>.
- [8] M. Ahmadi, M.H. Mousavi, H. Moradi, and K. Rouzbehi. “**A new approach for harmonic detection based on eliminating oscillatory coupling effects in microgrids**”. *IET Renewable Power Generation*, 17(14):3536–3553, 2023. DOI: <https://doi.org/10.1049/rpg2.12867>.
- [9] D.R. Nair, M.G. Nair, and T. Thakur. “**A smart microgrid system with artificial intelligence for power-sharing and power quality improvement**”. *Energies*, 15(15):5409, 2022. DOI: <https://doi.org/10.3390/en15155409>.
- [10] N. Gupta, A. Swarnkar, and K.R. Niazi. “**Distribution network reconfiguration for power quality and reliability improvement using Genetic Algorithms**”. *International Journal of Electrical Power & Energy Systems*, 54:664–671, 2014. DOI: <https://doi.org/10.1016/j.ijepes.2013.08.016>.
- [11] J. He, Y.W. Li, and F. Blaabjerg. Flexible microgrid power quality enhancement using adaptive hybrid voltage and current controller. *IEEE Transactions on Industrial Electronics*, 61(6):2784–2794, 2013. DOI: <https://doi.org/10.1109/TIE.2013.2276774>.
- [12] M.S. Mahmoud, N.M. Alyazidi, and M.I. Abouheaf. “**Adaptive intelligent techniques for microgrid control systems: A survey**”. *International Journal of Electrical Power & Energy Systems*, 90:292–305, 2017. DOI: <https://doi.org/10.1016/j.ijepes.2017.02.008>.
- [13] P. Ray and S.R. Salkuti. “**Smart branch and droop controller based power quality improvement in microgrids**”. *International Journal of Emerging Electric Power Systems*, 21(6), 2020. DOI: <https://doi.org/10.1515/ijeeps-2020-0094>.

- [14] B. Keyvani-Boroujeni, B. Fani, G. Shahgholian, and H.H. Alhelou. “**Virtual impedance-based droop control scheme to avoid power quality and stability problems in VSI-dominated microgrids**”. *IEEE Access*, 9:144999–145011, 2021. DOI: <https://doi.org/10.1109/ACCESS.2021.3122800>.
- [15] L.A. Paredes, B.R. Serrano, and M.G. Molina. “**FACTS Technology to Improve the Operation of Resilient Microgrids**”. In *2019 FISE-IEEE/CIGRE Conference-Living the energy Transition (FISE/CIGRE)*, pages 1–7, 2019. DOI: <https://doi.org/10.1109/FISECIGRE48012.2019.8984960>.
- [16] J. Qi, W. Zhao, and X. Bian. “**Comparative study of SVC and STATCOM reactive power compensation for prosumer microgrids with DFIG-based wind farm integration**”. *IEEE Access*, 8:209878–209885, 2020. DOI: <https://doi.org/10.1109/ACCESS.2020.3033058>.
- [17] W. Aslam, Y. Xu, A. Siddique, and F.M. Albatsh. “**Implementation of series facts devices SSSC and TCSC to improve power system stability**”. In *2018 13th IEEE Conference on Industrial Electronics and Applications (ICIEA)*, pages 2291–2297, 2018. DOI: <https://doi.org/10.1109/ICIEA.2018.8398092>.
- [18] O.J. Ewaoche and N. Nwulu. “**Design and Simulation of UPFC and IPFC for Voltage Stability under a Single Line Contingency: A Comparative Study**”. In *Proceedings of the International Conference on Industrial Engineering and Operations Management*, pages 27–29, 2018. DOI: <https://doi.org/10.46254/NA03.20180373>.
- [19] F. Li, M. Yu, Z. Li, J. Yuan, X. Yang, W. Zhang, and C. Zou. “**Summary of research on phase shifting transformer**”. In *Conference Proceedings of 2021 International Joint Conference on Energy, Electrical and Power Engineering: Component Design, Optimization and Control Algorithms in Electrical and Power Engineering Systems*, pages 103–110, 2022. DOI: <https://doi.org/10.1007/978-981-19-3171-0-9>.
- [20] B. Vyas, R.P. Maheshwari, and B. Das. “**Evaluation of artificial intelligence techniques for fault type identification in advanced series compensated transmission lines**”. *IETE Journal of Research*, 60(1):85–91, 2014. DOI: <https://doi.org/10.1080/02564602.2014.893767>.
- [21] P. Rao, M.L. Crow, and Z. Yang. “**STATCOM control for power system voltage control applications**”. *IEEE Transactions on power delivery*, 15(4):1311–1317, 2000. DOI: <https://doi.org/10.1109/61.891520>.
- [22] R. Sadiq, Z. Wang, C.Y. Chung, C. Zhou, and C. Wang. “**A review of STATCOM control for stability enhancement of power systems with wind/PV penetration: Existing research and future scope**”. *International Transactions on Electrical Energy Systems*, 31(11):e13079, 2021. DOI: <https://doi.org/10.1002/2050-7038.13079>.
- [23] Y. Lee and H. Song. “**A reactive power compensation strategy for voltage stability challenges in the Korean power system with dynamic loads**”. *Sustainability*, 11(2):326, 2019. DOI: <https://doi.org/10.3390/su11020326>.
- [24] Y. Han, H. Li, P. Shen, E.A.A. Coelho, and J.M. Guerrero. “**Review of active and reactive power sharing strategies in hierarchical controlled microgrids**”. *IEEE Transactions on Power Electronics*, 32(3):2427–2451, 2016. DOI: <https://doi.org/10.1109/TPEL.2016.2569597>.
- [25] E. Hashemzadeh, M. Khederzadeh, M.R. Aghamohammadi, and M. Asadi. “**A robust control for D-STATCOM under variations of DC-link capacitance**”. *IEEE Transactions on Power Electronics*, 36(7):8325–8333, 2020. DOI: <https://doi.org/10.1109/TPEL.2020.3026092>.
- [26] H.M. El Zoghby and H.S. Ramadan. “**Isolated microgrid stability reinforcement using optimally controlled STATCOM**”. *Sustainable Energy Technologies and Assessments*, 50:101883, 2022. DOI: <https://doi.org/10.1016/j.seta.2021.101883>.
- [27] N.K. Saxena, W.D. Gao, A. Kumar, S. Mekhilef, and V. Gupta. “**Frequency regulation for microgrid using genetic algorithm and particle swarm optimization tuned STATCOM**”. *International Journal of Circuit Theory and Applications*, 50(9):3231–3250, 2022. DOI: <https://doi.org/10.1002/cta.3319>.
- [28] S. Ranjan, D.C. Das, N. Sinha, A. Latif, S.S. Hussain, and T.S. Ustun. “**Voltage stability assessment of isolated hybrid dish-stirling solar thermal-diesel microgrid with STATCOM using mine blast algorithm**”. *Electric Power Systems Research*, 196:107239, 2021. DOI: <https://doi.org/10.1016/j.epsr.2021.107239>.
- [29] M.G. Yenealem, L.M. Ngoo, D. Shiferaw, and P. Hinga. “**Management of voltage profile and power loss minimization in a grid-connected microgrid system using fuzzy-based STATCOM controller**”. *Journal of Electrical and Computer Engineering*, pages 1–13, 2020. DOI: <https://doi.org/10.1155/2020/2040139>.
- [30] M.M. Hashempour and T.L. Lee. “**Integrated power factor correction and voltage fluctuation mitigation of microgrid using STATCOM**”. In *2017 IEEE 3rd International Future Energy Electronics Conference and ECCE Asia*, pages 1215–1219, 2017. DOI: <https://doi.org/10.1109/IFEEC.2017.7992215>.
- [31] Q. Song and W. Liu. “**Control of a cascade STATCOM with star configuration under unbalanced conditions**”. *IEEE Transactions on Power electronics*, 24(1):45–58, 2009. DOI: <https://doi.org/10.1109/TPEL.2008.2009172>.

- [32] Z. Miao, L. Piyasinghe, J. Khazaei, and L. Fan. “**Dynamic phasor-based modeling of unbalanced radial distribution systems**”. *IEEE transactions on power systems*, 30(6):3102–3109, 2015. DOI: <https://doi.org/10.1109/TPWRS.2014.2388154>.
- [33] Z. Shuai, Y. Peng, J.M. Guerrero, Y. Li, and Z.J. Shen. “**Transient response analysis of inverter-based microgrids under unbalanced conditions using a dynamic phasor model**”. *IEEE Transactions on Industrial Electronics*, 66(4):2868–2879, 2018. DOI: <https://doi.org/10.1109/TIE.2018.2844828>.
- [34] G. Tian, S. Wang, and G. Liu. “**Power quality and transient stability improvement of wind farm with fixed-speed induction generators using a STATCOM**”. In *2010 International Conference on Power System Technology*, pages 1–6, 2010. DOI: <https://doi.org/10.1109/POWERCON.2010.5666419>.
- [35] M.H. Mousavi and H.M. CheshmehBeigi. “**A brief review of methods for improving the performance of virtual synchronous generators under unbalanced conditions**”. In *2022 30th international conference on electrical engineering (ICEE)*, pages 630–635, 2022. DOI: <https://doi.org/10.1109/ICEE55646.2022.9827134>.
- [36] C.R. Amaya-Rodríguez and C.C. Chu. “**Laboratory-scaled STATCOM for unbalanced voltage sag mitigation by decoupled double synchronous reference current controllers**”. In *2013 IEEE International Symposium on Industrial Electronics*, pages 1–6, 2013. DOI: <https://doi.org/10.1109/ISIE.2013.6563617>.
- [37] M. Ahmadi, P. Sharafi, M.H. Mousavi, and F. Veysi. “**Power quality improvement in microgrids using statcom under unbalanced voltage conditions**”. *International Journal of Engineering*, 34(6):1455–1467, 2021. DOI: <https://doi.org/10.5829/ije.2021.34.06c.09>.
- [38] A. Meligy, T. Qoria, and I. Colak. “**Assessment of Sequence Extraction Methods Applied to MMC-SDBC STATCOM under Distorted Grid Conditions**”. *IEEE Transactions on Power Delivery*, 37(6):4923–4932, 2022. DOI: <https://doi.org/10.1109/ISIE.2013.6563617>.
- [39] A. Yazdani and R. Iravani. “**Voltage-sourced converters in power systems: modeling, control, and applications**”. *John Wiley & Sons*, 2010. DOI: <https://doi.org/10.1002/9780470551578>.